

PERFORMANCE CHARACTERIZATION OF THE VAPORIZING LIQUID MICRO-THRUSTER (VLM)

Juergen Mueller , John Ziemer, Amanda Green, and David Bame

*Jet Propulsion Laboratory
California Institute of Technology
Pasadena, CA 91109*

A Vaporizing Liquid Micro-Thruster (VLM) microfabricated thruster was tested on water propellant on a thrust stand and performance data obtained. Thrust values between 50 – 280 μN , thrust-to-power ratios of up to 200 $\mu\text{N}/\text{W}$ at power levels of 1- 1.5 W were measured. Mass flow rates ranges between 100 to just under 300 $\mu\text{g}/\text{s}$. Dividing measured thrust values by measured mass flow rates yielded specific impulse values around 100 sec. Specific impulse values have to be viewed with caution, however, as they are based on very difficult low mass flow measurements at low feed pressures. Different thruster operating modes were observed, based on whether the VLM chip ingested vapor, liquid water, or two-phase flow. Two-phase flow ingestion led to pulsing of the thruster, while all vapor or liquid ingestion led to a steady , quiescent thrusting mode. The liquid ingestion mode led to higher thruster performances due to enhanced heat transfer from the chip into the liquid. Even the quiescent thruster operating mode for liquid propellant ingestion was difficult to attain and maintain, however, and future VLM and feed system modifications will be required. Several design changes were easily identifiable.

I. INTRODUCTION

Microspacecraft have stirred interest within the aerospace community for the better part of the last decade. Recently, microspacecraft architectures have been inserted into actual mission designs and studies. The National Aeronautics and Space Administration's (NASA's) Space Science Sun-Earth-Connection (SEC) Theme, for example, is planning a large constellation mission termed Magnetic Constellation Missions (MagCon) consisting of dozens of very small (10 kg total wet mass) spacecraft, called nanospacecraft, performing tensor mapping of Earth's magnetic field (Fig. 1)¹. Such large constellations of spacecraft are only feasible if very small spacecraft are used in order to keep total launch masses reasonable and launch cost affordable. Other SEC missions under study include derivatives and follow-on missions to MagCon, such as "Dayside Boundary Condition" and "Inner Magnetospheric Constellation"¹. Other examples of microspacecraft may be found in the defense area. The Department of Defense (DoD) has an interest in spacecraft constellations for Earth observation, ranging from 100-kg spacecraft in the TechSat 21 constellation (Fig. 2) to "picosats", i.e. 1 kg total wet mass spacecraft, studied by the Defense Advanced Research Projects Agency (DARPA) (Figs. 3 and 4).



Fig. 1: Magnetic Constellation (MacCon) Mission Concept (NASA Sun-Earth-Connection Theme)¹



Fig. 2: AF TechSat 21 Mission Concept

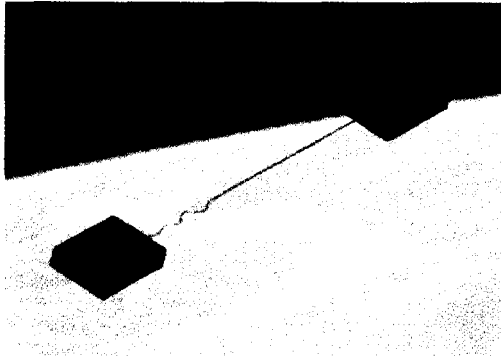


Fig. 3: DARPA 1-kg Picosat Spacecraft (Artist's conception)



Fig. 4: Aerospace Corp./JPL Picosat Launch on STS-113 (Dec. 2002)

In the case of such small spacecraft, significant propulsion system size and mass reduction is required for these subsystems to fit within the greatly reduced mass and size envelope. In addition thrust and impulse bit capabilities may also be required to be very small depending on spacecraft mass and required pointing accuracy. Table 1 lists potential impulse bit requirements and required thrust levels for slew ($180^\circ/\text{min}$) for three generic cubical spacecraft of 1, 10, and 20 kg mass, respectively². Shown are different pointing (dead-band) requirements and time intervals between thruster firings. In general, longer time required between thruster firings (e.g. to not disturb measurements, or to conserve propellant) requires lower rotation rates of the spacecraft as it drifts through the deadband, and, hence, a smaller impulse bits imparted onto the spacecraft is needed. As can be seen, required impulse bits may range from the mNs-range for larger craft having relatively coarse attitude requirements, into the μNs -range and possible even nNs range for very tight pointing requirements and very small spacecraft. On the other hand, slew rate requirements may drive required thrust levels into the milli-Newton range for 10-kg class spacecraft, while less than 0.1 mN maybe sufficient for 1-kg spacecraft. Note that these values are dependent on slew rate requirements, which are highly mission dependent, and may be different from the ones assumed here.

In addition to microspacecraft-based constellation missions, formation flying missions are being studied at NASA as well as the European Space Agency (ESA). Such formation flying missions essentially represent a single, large space-based instrument, such as an interferometer, distributed amongst several spacecraft. This approach requires these spacecraft to be held in a precisely controlled formation, which in turn translates into a requirement for very small, low-noise thrust levels. Table 2 lists thrust, noise and impulse bit requirements for some of the formation flying missions currently under consideration, showing the very small thrust requirements ion the micro-Newton to milli-Newton range. At present, only a very limited number of propulsion devices appear able to meet these requirements, such as colloid, Field Emission Electric Propulsion (FEEP), Pulsed Plasma Thrusters (PPTs) and some other, novel micro-thrust devices.

Table 1: Representative Attitude Control Requirements for Microspacecraft

S/C Mass (kg)	S/C Typ. Dimension* (m)	Moment of Inertia (kg m ²)	Required Impulse Bit (Ns)						Minimum Thrust for Slew (mN)
			17 mrad (1°)		0.3 mrad (1 arcmin)		0.02 mrad (5 arcsec)		
			20 s	100 s	20 s	100 s	20 s	100 s	
1	0.1	0.017	1.4×10^{-4}	2.9×10^{-5}	2.5×10^{-6}	5.1×10^{-7}	1.7×10^{-7}	3.4×10^{-8}	0.06
10	0.3	0.150	4.3×10^{-4}	8.5×10^{-5}	7.5×10^{-6}	3.0×10^{-6}	1.0×10^{-6}	1.0×10^{-7}	1.75
20	0.4	0.533	1.1×10^{-3}	2.3×10^{-4}	2.0×10^{-5}	4.0×10^{-6}	1.3×10^{-6}	2.7×10^{-7}	4.65

- Assume cubical spacecraft shape

Table 2: Some Formation Flying Requirements

Parameter	LISA/ST-7	TechSat 21	TPF
Thrust	1-20 μN	2 mN ('03) 40-200 μN (follow-on)	0.1 N (reformation) ~ μN (pointing)
Thrust Noise	0.1 μN		
Impulse Bit	-	2 mNs ('03) 2 μNs (follow-on)	

Novel thruster developments meeting these very low thrust and impulse bit requirements, as well as, in the case of microspacecraft constellations, size and weight requirements are therefore needed. One such thruster concept is the Vaporizing Liquid Micro-Thruster (VLM), explored at the Jet Propulsion Laboratory (JPL) and presented in this paper. This entirely microfabricated thruster device is primarily targeted for use in very small microspacecraft constellations to serve as an attitude control thruster. The thruster vaporizes a suitable propellant, such as water, ammonia, or others, stored compactly in its liquid phase on demand for thrust generation. Liquid propellant storage significantly reduces system mass and size requirements over high pressure gaseous storage, and reduces propellant leakage concerns. The thruster chip itself is fabricated using Microelectromechanical Systems (MEMS) technologies into silicon material (Fig. 5 and 6) and will ultimately be tightly integrated with a micro-piezovalve³ into a very compact thruster module. Figure 7 shows a crude precursor of such a thruster module, used in current testing activities prior to availability of the piezovalve. It features a solenoid valve made by the Lee company, epoxy bonded to the thruster chip via a Pyrex thermal stand-off featuring an internal feed capillary. This set-up serves ground-testing purposes of the VLM thruster chip only. It is too fragile to be considered a bread-board unit. In this paper, we will present recently obtained thruster performance data, such as thrust, specific impulse, power and propellant flows with test articles of the type shown in Fig. 7.

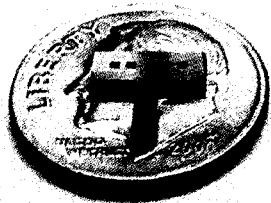


Fig. 5: Vaporizing Liquid Micro-Thruster (VLM). (US Dime for scale).

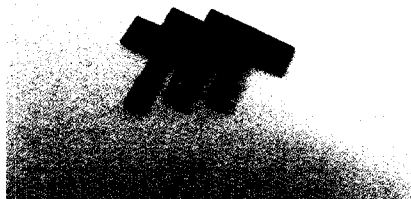


Fig. 6: VLM Thruster Chip Components. Observe nozzle contour on two left-most components.



Fig.7: VLM Test Article mounted to Lee Solenoid Valve via Pyrex Thermal Stand-Off.

II. THE VAPORIZING LIQUID MICRO-THRUSTER

Concept

The Vaporizing Liquid Micro-Thruster (VLM) concept went through various design iterations over the last few years. The most recent design, proposed by Chakraborty, is T-shaped to thermally isolate the heater section from the bulk of the chip (Fig. 5). It consists of a laminate of three chips (Figs. 6 and 8). The two outermost layers contain thin-film deposited gold heaters, spaced apart by a third spacer-chip. The chips are joined via a gold thermal compression bond, using a gold layer deposited in the same fabrication step as the heaters. Liquid propellant, in this case water for safety reasons, is pressure-fed between the heater strips, vaporized, and expanded through a micro-nozzle. The nozzle has a quasi-2-D conical (30° full angle) contour machined by Deep Reactive Ion Etching (DRIE) into the center chip together with the heater channel featured in the same chip. The two heater chips seal the channel and nozzle at the top and bottom. The chip ejects propellant sideways. Different chip geometries are being studied. Results presented here are for a chip featuring a heater channel length of 7.8 mm, and channel width of $700\ \mu\text{m}$ and a channel height of $300\ \mu\text{m}$. The nozzle is about $50\ \mu\text{m}$ wide, and has the same height as the heater channel.

It should be noted that silicon, although the fabrication material of choice from a microfabrication point of view due to substantial MEMS heritage, is not the best material from the standpoint of thruster operation. This is because silicon is a very good heat conductor (about $150\ \text{W/m K}$), which leads to heat losses from the thrust chamber. Since novel MEMS fabrication techniques using more suitable materials are difficult and time-consuming to develop, insulation of the chip was aimed for by integrating it via a thermal stand-off made from Pyrex to a suitable valve (see Fig. 7). Future integration of the VLM will feature a silicon machined piezo-valve, and a more rugged thruster module design. The set-up shown in Fig. 7 is for VLM test purposes only.

A key design target of the VLM concept is to vaporize liquid propellants, rather than merely heat gaseous propellants in an extension of the cold gas thruster concept. Although a higher power penalty will have to be paid for propellant vaporization, the use of liquid propellants translates into key system benefits, which are particularly crucial to microspacecraft design. These include smaller system size and weight through use of a lighter-weight, and smaller propellant tank than would have to be used to store an equivalent gaseous propellant mass. Leakage concerns, often raised with the storage of high-pressurant gaseous propellants, are also significantly less severe for liquid propellants, potentially increasing reliability of the system. At present the VLM thruster uses water propellant for safety reasons in laboratory testing. Water is also storable at fairly high densities. In principle, any liquid propellant can be used that can be vaporized at significantly low power levels. Ammonia, for example, is another propellant candidate considered, having about half the heat of vaporization than water.

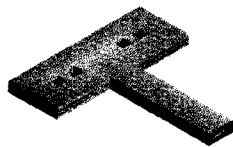


Fig. 8(a): VLM with 2-D Nozzle

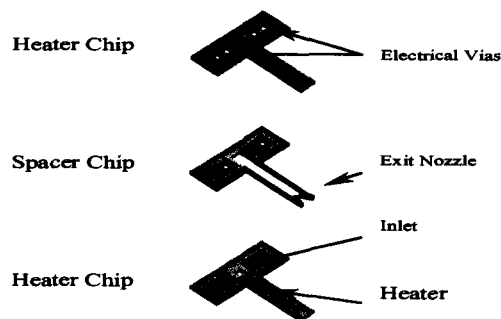


Fig. 8(b): Exploded View of VLM

Previous and Related Research:

The VLM concept shown in Fig. 8 is the latest version of a concept that was originally proposed at JPL in 1996. Earlier chip versions were larger, and featured heater channel sections that embedded in a rectangular chip design^{4,5}. The high heat conductivity of silicon lead to high heat losses from the chip, resulting in most of the power supplied to the chip to be lost to the surroundings. Early power requirements to achieve complete water vaporization under laboratory conditions ranged between 2-8 W⁵. A VLM version featuring heater fins inserted into the flow path was investigated as well⁵. However, diagnostics to measure the very low sustainable water flow rates was poor, and measurements remained inconclusive. The current T-shaped design provided better thermal insulation of the heater section, and was subsequently tested on a JPL thrust stand, originally supplied by Princeton University⁶. In early tests of this device, 30 – 120 $\mu\text{N}/\text{W}$ were measured at power levels of just over 1 W^{6,7}. As will be seen in this paper, the thrust-to-power ratio was almost doubled since by adjusting the operating conditions, resulting in thrust levels as high as 280 μN at power levels of 1.4 W.

The JPL VLM concept did not remain the only thruster concept of its kind. Previously to the JPL VLM concept, a micromachined resistojet using gaseous propellants had been proposed by Janson at Aerospace Corp.^{8,9}. In this concept, propellant flows over and under a suspended membrane that features the heater element for insulation. No test data are know to the authors. Wallace, at UC Davis, explored a VLM concept in a student project based on the JPL design, but incorporating several modifications, such as external heaters and a one sided heater geometries^{10,11}. Water vaporization was achieved at flow rates of 0.09 cc/sec and 5 W input power. Thrust values between 0.15 and 0.46mN were measured by determining the deflection of a pendulum to which the thruster was mounted¹¹. This work has not been continued according to the knowledge of the authors. A Chinese version of a water-fed vaporizing liquid micro-thruster, similar in design to earlier JPL versions, but featuring only one heater, was presented in 1999¹². Up to 2.9 μN peak thrust and an impulse bit of 0.2 μNs were measured by determining the deflection of a cantilevered beam placed into the thruster exhaust via Laser Doppler-shifts. The accuracy of this method was not given. A Laser Doppler velocimetry approach determined exhaust velocities of 8.5 m/s average and 28 m/s peak. It is unclear whether complete vaporization occurred. The thruster supposedly operated in a pulsed mode at a very high 48 W. Bayt and Breuer¹³ as well explored a resistojet design based on a fin-heater design. A very similar concept is being studied in Sweden at the Angstrom Institute of the University of Uppsala¹⁴. This concept is initially based on the usage of cold gas propellants, building on significant development efforts in that area. The Swedish work is the only one still ongoing of the activities reviewed so far according to the knowledge of the authors. Finally, more recently the Surrey Space Centre in England is embarking to investigate a miniaturized low-power resistojet using water propellant as well¹⁵. The concept, although not MEMS-based in its current design, is assumed to use the same Lee valve as shown in Fig. 7 as a thruster valve. Surrey is interested in this concept for its "Palmsat" 1-kg microsatellite concept due to cost efficiency and high-density propellant storability of a water-based propulsion system.

III. EXPERIMENT

Experimental Set-Up

The thruster chip is integrated with a thruster valve, manufactured by the Lee Company, via a Pyrex thermal stand-off as shown in Fig. 7. This assembly is then integrated with a propellant feed system and flow measurement diagnostics on a micro-Newton thrust stand (Figs. 9 and 10). Water propellant is stored in a pressurized electropolished tank. Adjusting feed pressure (Argon gas is sued in this case due to availability) will change the flow rate supplied to the thruster. The flow is routed through a micro-capillary with an inner diameter of 0.005" and a length of 250 mm before entering the thruster chip assembly. Pressure transducers located upstream and downstream of the capillary allow measurement of the pressure differential across the capillary during propellant flow. The capillary is calibrated prior to testing by weighing the amount of water that has flown through the capillary at a given pressure differential over a given time. A known pressure differential during thruster testing will then allow for the determination of the mass flow rate supplied to the thruster chip. Using thrust and measured flow rate, the specific impulse can be calculated.

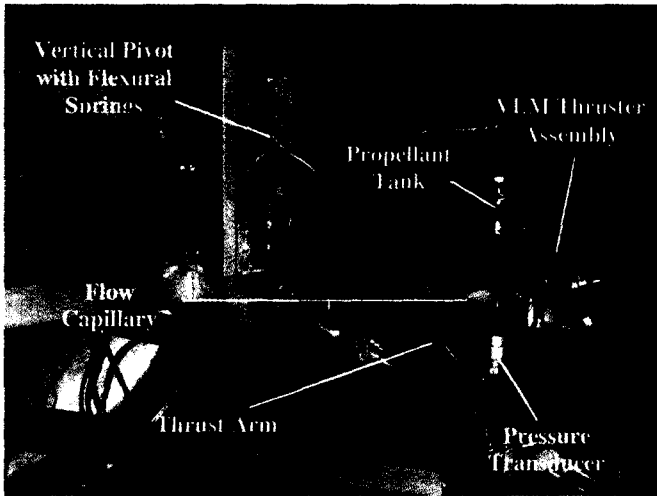


Fig. 9: VLM Mounted on JPL Micro-Newton Thrust Stand

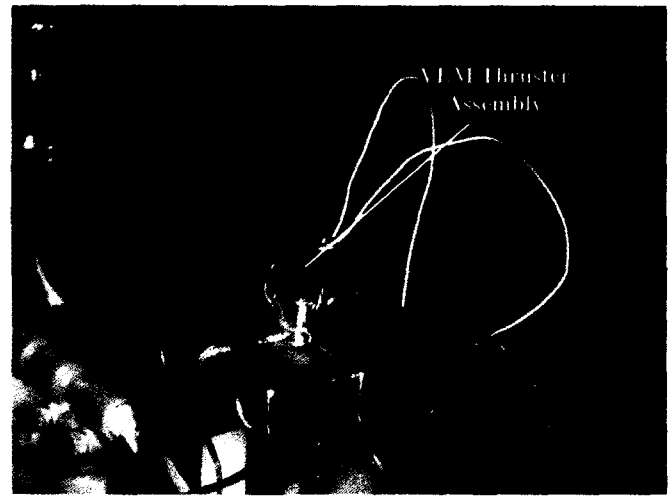


Fig. 10: Close-Up of VLM/valve Assembly Mounted on Thrust Stand

Thruster and Lee valve temperature are being measured via thermocouples attached to the VLM chip (at the T-joint between heater section and base of the chip) and valve, respectively. Heater power to the chip is measured of the heater power supply. All data, incl. the pressure levels upstream (feed pressure) and downstream (thruster inlet pressure) of the capillary and the thrust are recorded via a Labview data acquisition system. A video camera set at high magnification allowed a detail viewing and recording of thruster behavior, incl. observation of the flow through the thermal Pyrex stand-off. The nature of this flow, whether in its liquid phase, two-phase, or vapor, was found to have a significant effect on thruster operation.

Measuring performances of the VLM devices discussed in this paper requires extremely accurate thrust measurement capability. This is accomplished with a micro-Newton thrust stand with a resolution of $0.5 \mu\text{N}$ or better⁶. The design is based on thrust stand technology originally developed at Princeton University, which in turn was based on an earlier design by Fairchild¹⁶. The thruster is mounted onto a horizontally swing thrust arm, attached via two flexural springs at two pivot locations to a vertical support arm (see Fig. 9). The vertical arm in turn is attached to an L-shaped structure that can be leveled to eliminate gravity effects acting on the swinging thrust arm. The thrust arm deflects until the restoring force of the flexural springs and the thrust force equal. Thrust arm deflection can be measured via a Linear Variable Differential Transducer (LVDT) with a sub-micron resolution, resulting in about $0.5 \mu\text{N}$ thrust resolution. A damping circuit damps the natural oscillations of the thrust stand (typically with a 1- 10 s period) upon thrust actuation. The thrust stand is calibrated by hitting it with a force transducer mounted to a swing-arm. The impulse bit recorded by the force transducer can be calibrated against the deflection of the thrust arm, and important thrust stand parameters, such as effective mass, and spring constant be calculated⁶.

Results

Test results were obtained for a thruster chip with a hea channel length of 7.8 mm, as described in Section II. Several different modes of operation were observed with this VLM assembly, shown in Figs. 11-14. Each of the figures shows a thrust trace for a particular test run, along with thruster chip and valve temperature traces. In the case of Fig. 11, large thrust oscillations can be observed. The propellant flow entering the chip could be observed to be mostly vapor when observed through the Pyrex capillary. This is believed to be due to the low thruster inlet pressure (about 1.57 – 1.85 psia measured during the latter half of the test run) in this case and the Lee solenoid valve acting as a heating source upstream. The valve temperature is about 65°C without flow passage due to heating losses from the thruster chip, which itself is about 164°C prior to opening the valve. Once the valve is opened, as indicated in Fig. 11 by the sharp increase in thrust from its zero level, both chip and valve temperature drop as a result of the propellant flow cooling the flow passages and components it passes through. While the valve temperature drops, the flow is not high enough (merely $100 - 140 \mu\text{g/s}$, accounting for the flow oscillations) to cool it below 50°C . At the measured valve temperature of $50 - 52^\circ\text{C}$ near the end of the run, the

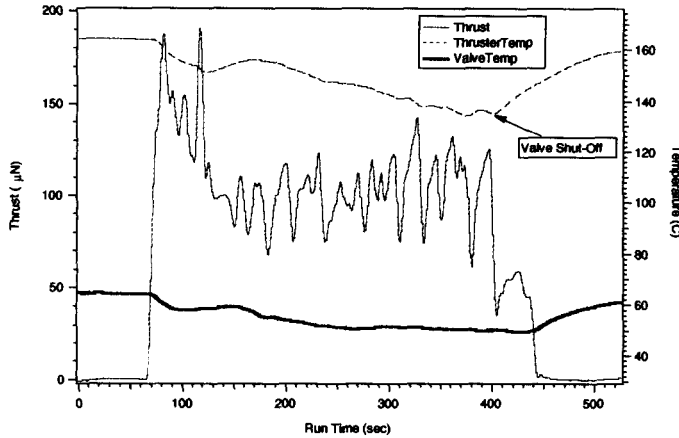


Fig. 11: Thrust and Temperature Curves for Run #19 (61 – 140 μN thrust, 1.07 W input power, 99–140 $\mu\text{g/s}$ mass flow)

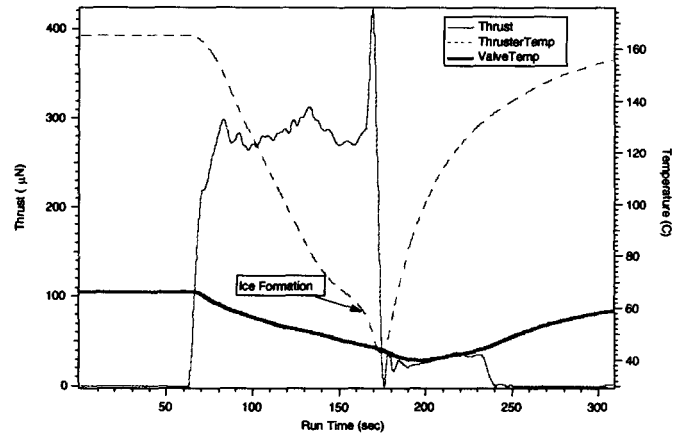


Fig. 12: Thrust and Temperature Curves for Run #22 (272 μN thrust, 1.27 W input power, 203 – 221 $\mu\text{g/s}$ mass flow just prior to icing).

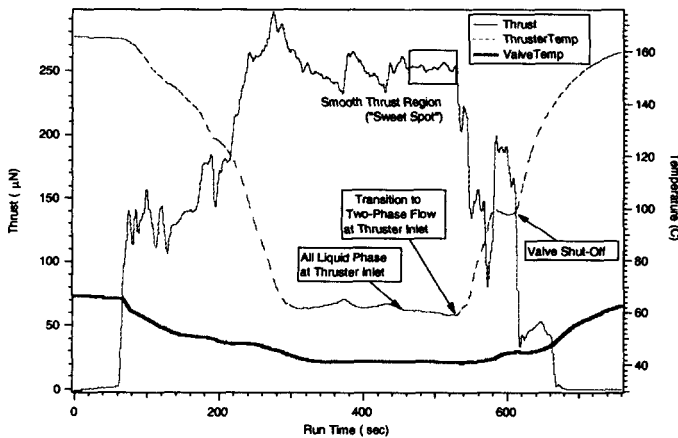


Fig. 13: Thrust and Temperature Curves for Run #21 (248–252 μN thrust, 1.28 W input power, 229–233 $\mu\text{g/s}$ mass flow in “sweet spot” mode)

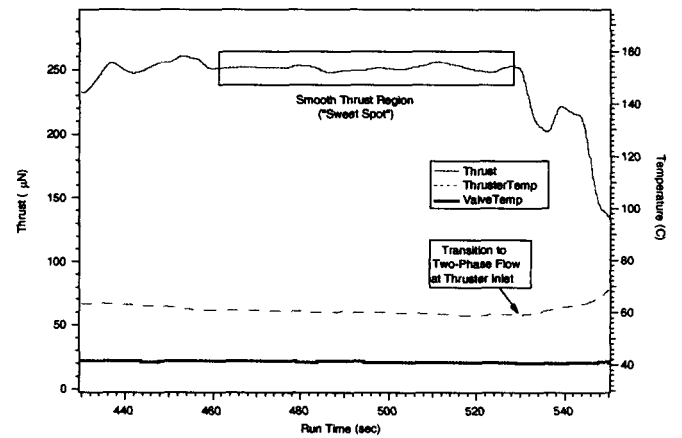


Fig. 14: Close-Up of “Sweet Spot” Mode in Figure 13

vapor pressure of water would be 1.79 – 1.97 psia. This is higher than the thruster inlet pressure given above. Hence flow vaporizes inside the valve. This vaporization does not appear to be complete, leading to pressure oscillations and subsequent mass flow and thrust oscillations. Clearly, this is not a desired mode of VLM operation.

In the case depicted in Fig. 12, a much higher flow rate is fed into the thruster at a chip temperature of 165 $^{\circ}\text{C}$ prior to valve opening, i.e. comparable to the case in Fig. 11. This higher flow cools the chip much more rapidly, as indicated by the precipitous fall of thruster temperature in Fig. 12. While initially, when valve temperatures are still high, flow vaporization occurs in the valve as in the case shown in Fig. 11, causing similar pulsing action by the thruster, the valve temperature drops so fast that water vaporization pressures finally are lower than feed pressures (about 1.95 – 2.03 psia thruster inlet pressure measured towards the end of this run) as valve temperatures drop to 46–48 $^{\circ}\text{C}$, and liquid water enters the chip. However, thruster chip temperatures also have dropped below values to sustain vaporization inside the chip, and once dropping below approximately 58 $^{\circ}\text{C}$, water exits the chip, quickly freezes at the nozzle exit of the thruster chip in the vacuum of the test chamber, which dramatically cools the chip further, as seen by the downward bend in the thruster temperature curve of Fig. 12. The valve is closed shortly afterward to avoid excessive ice build up at the nozzle exit, as indicated by

the sharp drop in thrust and chip temperature recovery due to lack of further flow cooling after valve closure. Obviously, this is not a desirable operating mode for the VLM either.

In Fig. 13 finally, the feed pressure, and hence flow, have been adjusted in such a way, that a thruster operating mode ensues where water vaporization is no longer possible inside the valve due to a high enough feed pressure, while icing is prevented due to the flow (and feed pressure) being low enough to avoid excessive chip cooling. However, as can be seen when examining Fig. 13 closer, this mode only occurs over a relatively short section of the test run. At first, while valve temperatures are still high (starting conditions are again 65 °C valve temperature and 165 °C thruster chip temperature prior to flow), flow vaporization occurs inside the valve, leading to two-phase flow ingestion by the thruster and the previously observed resulting thruster oscillations. The valve temperature finally cools to about 41 C, holding steady at this point. The thruster inlet pressure in this case is about 1.69 – 1.73 psia at this stage of the test run. This is higher than the vaporization pressure of water (1.13 psia) for the given valve temperature, and, hence, vaporization inside the valve ceases.

From this point forward, all liquid water enters the thruster chip. In this mode, thruster oscillations quite down significantly, and the thruster enters a smooth thrusting region, loosely termed “sweet spot” mode here. The “sweet spot” mode is enlarged in Fig. 14. Thrust in this operating range ranges between 248 – 256 μN , with an average thrust value of 252 μN at a standard deviance of 1.72 μN , or less than 1% of the total thrust. Unfortunately, as was the case in other test runs, this mode could only be maintained for a little over a minute. In some cases, icing occurred afterward at the thruster exit, in the case in Fig. 13 and 14, the flow resorted back to a state of vaporization inside the valve, two-phase flow ingestion by the thruster and hence flow and thrust oscillations.

It is unclear what caused this transition back to the oscillating vapor-phase mode. Valve temperature can be seen to increase slightly again. It is possible that the pressure transducers located further upstream may have caused flow vaporization. These transducers have been observed to be at a temperature of about 40 °C after vacuum chamber opening, and may thus be even hotter when operating in vacuum. No temperature data are available for these components. Vapor ingestion by the valve would reduce cooling, a raise in valve temperature, which might possibly trigger two-phase flow downstream inside the capillary leading up to the thruster inlet again.

It is obvious from studying Fig. 13, that while exhibiting a short section of fairly quiescent thrusting behavior, the current VLM design and flow system does not represent a practical solution for an operational propulsion system. The “sweet spot” modes are too difficult to attain, require too careful an adjustment of flow and feed pressure, and it is unacceptable to wait several minutes, as in the case of Fig. 13, to encounter this mode. However, the observed flow behavior, together with the quantitative data obtained on thruster inlet pressures, valve temperatures, and thrusting behavior offer some fairly simple, potential solutions to this problem.

It appears, that eliminating heat sources upstream of the thruster chip, and/or increasing the thruster inlet and feed pressures will prevent vaporization and two-phase flow upstream of the thruster, and thus should allow for the quiescent thrusting mode as shown in Fig. 14 shortly after thruster actuation and be maintainable over a wider operating range with respect to flow rates, feed pressures and thrusts. This may be achieved via flow restrictors placed upstream of the thruster chip, likely to be micromachined and integrated with the chip design, as well as the use of a lower power valve, such as the intended piezovalve for use with this thruster. These changes will be implemented next in the VLM development program.

Another change to be implemented is the reduction of “dribble volume”, i.e. the flow passage volume downstream of the valve seat. Too large a dribble volume will lead to a long time required for emptying the thruster of residual propellants in the flow lines after valve closure. Ultimately, this will lead to poor impulse bit performance. The emptying-out process can be recognized in Figs. 11-13 as the final “hump” in the thrust trace after valve shut-off, and is shown for the case of Fig. 13 enlarged in Fig.15. A little over a minute passes before a thrust level of zero is reached after valve shut down. Shallower and narrower heater channels, shorter if possible while still achieving complete vaporization, will be studied to reduce this time and the associated impulse bit.

In the meantime, the thruster performance data obtained during the quiescent “sweet spot” thrusting modes of the case shown in Figs. 13 and 14, as well as others not shown, give an indication of thruster performances that may ultimately be achieved in a more steady operating mode once these changes are implemented. Table 3

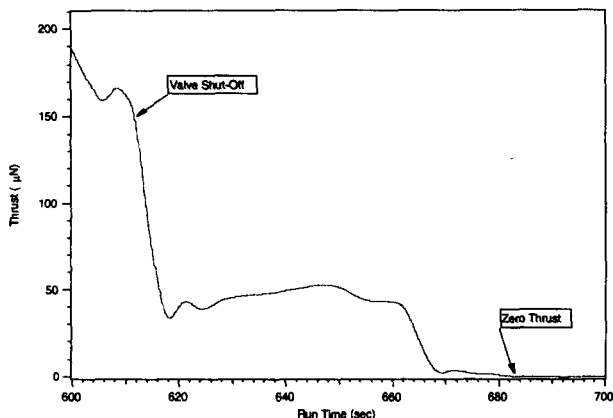


Fig. 15: “Dribble Volume” Effect after Thruster Shut-Down in Run 21

shows two of these cases, of which one is shown in Figs. 13 and 14. Also listed in Table 3 is a case where pure vapor entered the thruster chip, also leading to a fairly quiescent thrusting mode, yet at much reduced performances due to the decreased heat transfer from the heaters to the propellant in the gas phase. Thruster performances are quite impressive. Thrust levels in the range of 250 – 280 μN were measured and thrust-to-power ratios reach 200 μN/W. Mass flow rates are extremely small, 0.2 – 0.3 mg/s. These values reveal the difficulties encountered in measuring them. Similarly, since specific impulse is derived from thrust and mass flow measurements, determining this parameter was extremely difficult. The data show Isp values as high as 100 sec and above. This is about twice as high as the sonic speed calculated based on the measured chip temperature.

It is unclear at this point, whether the nozzle actually had such an effect on the specific impulse, or whether the Isp data are wrong. As mentioned, the specific impulse was determined by dividing measured thrust by measured mass flow rate. The flow rate was calibrated by weighing the water that flowed through a capillary during a given time. Calibrations were performed before and after test runs, and found to be within 10% of each other. However, the calibration had to be performed at atmospheric pressure. While for the same pressure differential across the capillary the same amount of flow should pass through it, the test runs were performed at much lower feed pressures inside the capillary. As mentioned above, the pressure transducers located just upstream and downstream of the capillary operated at temperatures of 40 °C or higher. At these temperatures, and feed pressures of 2 psia or less, vapor may have been generated. However, while the lower viscosity of vapor would lead to a volume flow increase for a given pressure difference, mass flow actually would decrease due to the much larger decrease in density¹⁷. Thus, vapor ingestion inside the cavity should have underestimated Isp when using calibrated liquid flow rates, not overestimated them. Nonetheless, specific impulse values should be considered very preliminary at this point due to the very difficult low mass flow measurements, and will be subject to further study.

IV. CONCLUSIONS

A VLM micro-thruster was tested on a thrust stand and key performance data were obtained. Different thruster operating modes were observed. Depending on two-phase flow on the one hand, or pure vapor or liquid phase flow entering the thruster chip, pulsing or steady thruster operation was noted, respectively. Too high a flow for a given power level led to rapid cooling of the chip, and subsequent ice formation at the nozzle exit. The steady operating mode with liquid propellant ingestion is the preferred thruster operating mode due to higher

Table 3: Sample of VLM Thruster Performance Data during “Sweet Spot” Mode

Parameter	Run 21	Run 31	Run 20
Thrust (μN)			
Avg.	252	279	53
Max.	256	281	54
Min.	248	278	51
Std. Deviation	1.7	0.46	0.7
Isp (s) (preliminary)			
Avg.	108	98	49
Max.	110	99	53
Min.	107	97	46
Std. Deviation	0.9	0.5	2.4
Power (W) (Avg.)	1.28	1.44	1.03
Thrust/Power (μN/W) (Avg.)	196	194	51
Mass Flow (μg/s) (Avg.)	233	284	108
Comments	All liquid at inlet	All liquid at inlet	All vapor at inlet

thruster performances over the all vapor mode. However, at present this mode is difficult to attain and maintain since it occurs only over a very narrow operating range with respect to feed pressure. Future VLM design iterations may feature flow orifices at the thruster entrance and low-power piezovalves to eliminate vaporization and two-phase flow conditions upstream of the thruster. In those cases, the performance data obtained during the brief quiescent thrusting modes may be representative for future VLM designs. Thrust values so far range from 50 – 280 μN at thrust-to-power levels of 200 $\mu\text{N}/\text{W}$. Specific impulse values were measured to be around 100 sec, but are based on very difficult low mass flow measurements at low feed pressures, and thus have to be viewed with caution at this point.

V. ACKNOWLEDGEMENTS

The authors would like to thank Dr. Leon Alkalai of the Micro/Nano Spacecraft Element, Dr. Jesse Leitner of the Revolutionary Spacecraft Systems task, and Dr. Chris Moore of the NASA Enabling Concepts and Technologies (ECT) program for supporting this work. The research described was carried out at the Jet Propulsion Laboratory, California Institute of Technology, under a contract with the National Aeronautics and Space Administration.

VI. REFERENCES

- ¹Sun-Earth Connection Roadmap 2003-2028, NASA, Sept. 2002, http://sec.gsfc.nasa.gov/sec_roadmap.htm
- ²Mueller, J., "A Review and Applicability Assessment of MEMS-Based Microvalve Technologies for Microspacecraft Propulsion", *Micropropulsion for Small Spacecraft*, Progress in Astronautics and Aeronautics, Vol. 187, edited by Micci, M. and Ketsdever, A., AIAA, Reston, VA, 2000, Ch. 19.
- ³Yang, E.H., Lee, C., Mueller, J., and George, T., "Leak-Tight Piezoelectric Microvalve for High-Pressure Gas Micropropulsion", Proceedings, IEEE 16th Annual Int'l Conf. on Microelectromechanical Systems (MEMS), pp. 80-83, Jan. 19-23, 2003, Kyoto, Japan.
- ⁴Mueller, J., Tang, W., Wallace, A., Li, W., Bame, D., Chakraborty, I., and Lawton, R., "Design, Analysis, and Fabrication of a Vaporizing Liquid Micro-Thruster", AIAA Paper 97-3054, 33rd Joint Propulsion Conference, Seattle, WA, July 6-9, 1997.
- ⁵Mueller, J., Chakraborty, I., Bame, D., and Tang, W., "The Vaporizing Liquid Micro-Thruster Concept: Preliminary Results of Initial Feasibility Studies", *Micropropulsion for Small Spacecraft*, Progress in Astronautics and Aeronautics, Vol. 187, ed. by Micci, M. and Ketsdever, A., AIAA, Reston, VA, 2000, Ch. 8.
- ⁶Ziemer, J.K., "Performance Measurements Using Sub-Micro Newton Resolution Thrust Stand", IEPC Paper 01-238, 27th International Electric Propulsion Conference, Oct. 15-19, 2001, Pasadena, CA.
- ⁷Mueller, J., Marrese, C., Ziemer, J., Green, A., Yang, E.H., Mojarradi, M., Johnson, T., White, V., Bame, D., Wirz, R., Tajmar, M., Hruby, V., Gamero-Castaño, M., Schein, J., and Reinicke, R., "JPL Micro-Thrust Propulsion Activities", AIAA Paper 2002-5714, Nanotech 2002, Sept. 9-12, Houston, TX.
- ⁸Janson, S.W., "Chemical and Electric Micropropulsion Concepts for Nanosatellites", AIAA Paper 94-2998, 30th Joint Propulsion Conference, June 27-29, 1994, Indianapolis, IN.
- ⁹Janson, S.W., Helvajian, H., and Hansen, W.W., "Batch-Fabricated CW Microthrusters for Kilogram-Class Spacecraft", AIAA Paper 99-2722, 35th Joint Propulsion Conference, June 20-24, 1999, Los Angeles, CA.
- ¹⁰Wallace, A.P., Mukerjee, E.V., Yan, K., Smith, R.L., and Collins, S.D., "Design, Fabrication, and Demonstration of a Vaporizing Liquid Attitude Control Microthruster", Transducers'99 Conference, June 2-6, 1999, Sendai, Japan.
- ¹¹Mukerjee, E.V., Wallace, A.P., Yan, K.Y., Howard, D.W., Smith, R.L., and Collins, S.D., "Vaporizing Liquid Microthruster", *Sensors and Actuators*, 83 (2000), pp. 231-236.
- ¹²Ye, X., Tang, F., Ding, H., and Zhou, Z., "A Vaporizing Water Micro-Thruster", location of publication uncertain, likely Transducers'99 Conference, June 2-6, 1999, Sendai, Japan.
- ¹³Bayt, R. and Breuer, K., "Systems Design and Performance of Hot and Cold Supersonic Microjets", AIAA Paper 2001-0721, 39th Aerospace Sciences Meeting, January 8-11, 2001, Reno, NV.
- ¹⁴Köhler, J., Simu, U., Jonsson, K., Lang, M., and Stenmark, L., "Feasibility Demonstration of the Micropropulsion Cold Gas Thruster System", Proceedings of the 3rd Roundtable on Micro/Nano technologies for Space, ESA Publication WPP-174, pp.219-225, May 15-17, 2000, Noordwijk, The Netherlands.
- ¹⁵Baker, A.M., Gibbon, D., and Underwood, C., "Micropropulsion from SNAP to Palmsat: When does MEMS Become the Way Forward?", AIAA Paper 2002-5759, Nanotech 2002, Sept. 9-12, Houston, TX.
- ¹⁶Cubbin, E., Ziemer, J., Choueiri, E., and Jahn, R., "Pulsed thrust measurements using laser interferometry", *Rev. Sci. Instrum.* 68 (6), June 1997, pp. 2339 – 2346.
- ¹⁷Incropera, F. and De Witt, D., "Fundamentals of Heat and Mass Transfer", 2nd ed., Wiley&Sons, New York, 1985